THE ASTROPHYSICAL JOURNAL, 383:487–497, 1991 December 20

PLANETARY NEBULAE AS STANDARD CANDLES. VII. A TEST VERSUS HUBBLE TYPE IN THE NGC 1023 GROUP

ROBIN CIARDULLO
Department of Astronomy and Astrophysics, Penn State University, 525 Davey Lab, University Park, PA 16802
GEORGE H. JACOBY
Kitt Peak National Observatory, National Optical Astronomy Observatories,[1] P.O. Box 26732, Tucson, AZ 85726
AND
WILLIAM E. HARRIS
Department of Physics and Astronomy, McMaster University, Hamilton, Ontario, Canada L8S 4M1
Received 1991 April 24; accepted 1991 June 27

ABSTRACT

We present the results of an [O III] λ5007 survey for planetary nebulae in the NGC 1023 Group. In all, we detected 143 planetary nebula candidates: 110 in the SB0 galaxy NGC 1023 and 33 in the halo of the edge-on Sb spiral NGC 891. Using a statistically complete and homogeneous sample of planetary nebulae and the procedures described in previous papers in the series, we derive distances to these galaxies using the planetary nebula luminosity function (PNLF). After correcting for foreground extinction by using the estimated reddening values of Burstein and Heiles, we find the distance moduli for NGC 1023 and NGC 891 are 29.97 ± 0.14 and 29.97 ± 0.16, respectively. The similarity of these distances demonstrates the insensitivity of the PNLF to galaxy Hubble types and population age, and again confirms it as one of the best extragalactic standard candles.

Subject headings: galaxies: distances — galaxies: individual (NGC 1023, NGC 891) — galaxies: stellar content — luminosity function — nebulae: planetary

1. INTRODUCTION

Planetary nebulae (PNs) have recently been shown to be among the best extragalactic standard candles. Measurements in the Leo I Group (Ciardullo, Jacoby, & Ford 1989; hereafter Paper IV) and in Virgo (Jacoby, Ciardullo, & Ford 1990; hereafter Paper V) have demonstrated excellent internal consistency: although the galaxies observed in these clusters range in [Fe/H] from 0.15 to 0.41 and have colors which differ by 0.34 in $U - V$ and 2.2 in $m_{1550} - V$, no systematic behavior in the derived distances has been detected. More impressive have been the small external errors found for the PN surveys of M81 (Jacoby et al. 1989; hereafter Paper III) and the LMC (Jacoby, Walker, & Ciardullo 1990; hereafter Paper VI). In both these galaxies, the derived planetary nebula luminosity function (PNLF) distance is statistically indistinguishable from that found from the I band and infrared observation of Cepheids (see Freedman & Madore 1988; Welch et al. 1987; Feast & Walker 1987). In addition, the PNLF distances to the Leo I Group and Virgo are identical to those estimated from the Tully-Fisher method (Tully & Pierce 1989; Pierce & Tully 1988), and Pottasch's (1990) PNLF-based distance estimate of 8.1 kpc to the Galactic center is completely consistent with that determined by other methods (Reid 1989).

Nevertheless, the case for the invariance of the PNLF is not yet airtight. PNLF distances are based on a zero point determined in the bulge of M31, an Sb galaxy (Ciardullo et al. 1989; hereafter Paper II), and, although the measurements performed to date show complete agreement between the PN and Cepheid distance scales, these comparisons can be made only in the later type galaxies that have a substantial Cepheid population. Unfortunately, all the rigorous internal tests that have been applied to the PNLF have taken place in early-type galaxies. The reason for this is that under normal ground-based seeing conditions, the task of discriminating PNs from the high-excitation, compact H II regions of a distant galaxy is difficult. In an elliptical or S0 galaxy, few H II regions exist, and an occasional misidentification is acceptable, since it does not significantly alter the derived distance. However, in most late-type spirals, the number of H II regions far exceeds the number of detectable PNs, and an accurate measurement of the PNLF is nearly impossible. Thus, it is extremely difficult to study the systematic behavior of the PNLF across a wide range of Hubble types.

There is one class of spiral galaxy where PN surveys are effective, however. H II regions are Population I objects and are thus confined to the galactic disk; PNs, however, come from stars of all ages and are located not only in the plane, but in the bulge and halo as well. Thus, if a spiral is viewed edge-on, PNs can be separated from H II regions on the basis of location, and a homogeneous sample of objects can be formed by considering just those emission-line sources located above and below the galactic plane. A galaxy cluster which contains an edge-on spiral is therefore an excellent place to measure the change in the behavior of the PNLF with Hubble type.

In this paper, we test the dependence of the PNLF with population age and Hubble type by measuring PNs in two galaxies of the NGC 1023 Group—NGC 1023 itself, which is a large, H I–rich SB0 galaxy, and NGC 891, the edge-on Sb spiral that is often compared to the Milky Way (Osterbrock & Sharpless 1952; van der Kruit 1984). These two galaxies are an ideal pair for looking for systematic differences in the PNLF. At a distance of ~10 Mpc (Aaronson & Mould 1983), NGC

[1] Operated by the Association of Universities for Research in Astronomy, Inc., under cooperative agreement with the National Science Foundation.

1023 and NGC 891 are close enough so that the PNLF can be well-sampled, yet far enough away so that depth effects in the cluster are unimportant. Furthermore, there is no question that the galaxies are actually associated: group catalogs, such as those by de Vaucouleurs (1975), Huchra & Geller (1982), and Tully (1988) all unambiguously place the galaxies within a common cluster. Thus, if the PNLF distances to the two galaxies agree to within ~ 1 Mpc, which we adopt as the nominal size of the galaxy cluster, we will have good reason to believe that the PNLF dependence on Hubble type is negligible.

In § 2 of this paper, we describe our observations of NGC 1023 and NGC 891 and briefly review the steps required to extract [O III] $\lambda 5007$ magnitudes from CCD images. We also present the positions and magnitudes of 143 PN candidates detected in the group. In § 3, we select a statistically complete subset of these objects to define the PNLF. We then derive distances to the two galaxies and show that the PNLF yields internally consistent distances, even across a wide range of Hubble types. In § 5 we present the luminosity-specific PN density for NGC 1023 and show that a correlation exists between a galaxy's $U - V$ color and its PN population. We discuss this trend and suggest that the key factor in this relationship is age, and that younger systems produce more bright PNs. In § 6, we discuss the reality of the sharp truncation of the PNLF and present possible scenarios to explain the existence of overluminous PN candidates. We conclude by analyzing the implications of a constant PNLF and discussing its use in future distance determinations.

2. OBSERVATIONS AND REDUCTIONS

In 1989 October NGC 1023 and NGC 891 were surveyed for PNs by using the prime focus of the Kitt Peak 4 m telescope and the 800 × 800 TI2 CCD, which afforded a plate scale of 0".3 per pixel. The observing technique used was similar to that described in previous papers of the series. PNs were detected through a redshifted [O III] $\lambda 5007$ filter, with a central wavelength of 5014 Å and a full width half-maximum (FWHM) of 35 Å at the ambient temperature (11°C) in the converging beam of the telescope. A 279 Å wide (FWHM) off-band filter centered at 5290 Å served to define the galaxy continuum. The total on-band exposure time for each field was 2 hr and consisted of two 1 hr frames. The off-band frames were made from two 7 minute exposures. The off-band exposures typically went ~ 0.2 mag fainter than their on-band counterparts and thus ensured against possible misidentifications of objects at the frame limit. Typical seeing for all these frames was 1".

In both NGC 1023 and NGC 891 it is possible to confuse compact H II regions with PNs: NGC 891 is an edge-on Sb galaxy with emission filaments extending $\sim 45''$ out of the plane (Rand, Kulkarni, & Hester 1990) and NGC 1023 has a small Magellanic Cloud type irregular superposed on its disk (Capaccioli, Lorenz, & Afanasjev 1986). Thus, to guard against possible confusion with H II regions, we also imaged each field for 30 minutes through a 75 Å wide (FWHM) Hα filter (λ_c = 6590 Å in the converging beam of the telescope) and for 5 minutes in an off-band Hα filter (λ_c = 6194 Å; FWHM = 348 Å). A log of these Hα observations, along with those in the $\lambda 5007$ filter appears in Table 1. The regions surveyed within each galaxy are displayed in Figure 1.

PN candidates were identified and measured in a manner similar to that described in detail in the previous papers of the series. We began by spatially registering all the individual frames of each field using ~ 10 stars to define the coordinate system. We then combined the multiple on-band and off-band frames of each field and "blinked" the on-band [O III] $\lambda 5007$ sum against the off-band $\lambda 5290$ sum. Objects clearly visible on the on-band image, but absent on the off-band frame, were noted as possible PN candidates. We then confirmed these identifications by creating an [O III] $\lambda 5007$ difference picture and locating each candidate PN on this image.

TABLE 1

Summary of Observations

Field	Date	Filter	Exp (minutes)	Seeing
NGC 1023 East	1989 Oct 28	5014/30	120	0".9
NGC 1023 East	1989 Oct 29	6590/75	30	1".2
NGC 1023 West	1989 Oct 28	5014/30	120	0".9
NGC 1023 West	1989 Oct 29	6590/75	30	1".2
NGC 1023 Center	1989 Oct 29	5014/30	60	1".2
NGC 891 Center	1989 Oct 28	5014/30	120	1".0
NGC 891 Center	1989 Oct 30	6590/75	30	1".6

Once the initial PN candidate list was produced, we performed three additional tests to exclude contaminating objects. First, to remove cosmic rays and bad pixel events from the sample, we examined the image of each PN candidate on the individual frames which comprised the on-band sum. All but the faintest PNs were visible on both frames; cosmic-ray events, on the other hand, were typically bright on one frame, but absent on the other. By comparing the images on the individual frames, we were able to remove the spurious detections and detector anomalies from the candidate list.

After removing the cosmic rays, we next examined our sample for contaminating H II regions. This was done in two ways. First, we compared the radial profile of each PN candidate on the difference picture to the image point spread function (PSF) as determined from field stars on the on-band sum frame. Since PNs outside the Local Group always appear stellar, we immediately deleted all objects in the sample that appeared extended. We then examined each PN candidate's location on our Hα − $\lambda 6200$ difference picture. Because of the shorter exposure times, the wider filter bandpass (which was not well-centered on the group's systemic velocity), and the generally poorer seeing, our Hα frames did not go as deep as their $\lambda 5007$ counterparts. Nevertheless, the Hα images were still useful for detecting compact H II regions: because most H II regions are low-excitation objects (Hα/[O III] > 1), while all [O III] bright PNs have Hα/[O III] ≈ 0.3, true PNs in NGC 1023 and NGC 891 could not be seen on our Hα frames. Therefore, we deleted from the sample any object that was detectable in Hα.

With the cosmic rays and H II regions removed, 33 PN candidates remained in NGC 891 and 115 remained in NGC 1023. For the latter galaxy, we then applied one additional discriminant. Superposed on the west side of NGC 1023 is a Magellanic Cloud–type irregular galaxy containing several bright H II regions. To remove any doubt concerning PN identifications in this region, we deleted all candidate objects in this part of the galaxy. This left NGC 1023 with 110 PN candidates.

The equatorial coordinates of the PN candidates were calculated as in Paper V. First, we used a Tektronix 2048 × 2048 CCD at the prime focus of the Kitt Peak 4 m telescope to obtain a wide field (18'.4 × 18'.4) R band exposure of each galaxy. We then measured the astrometric coordinates of faint field stars on these frames by comparing their positions to

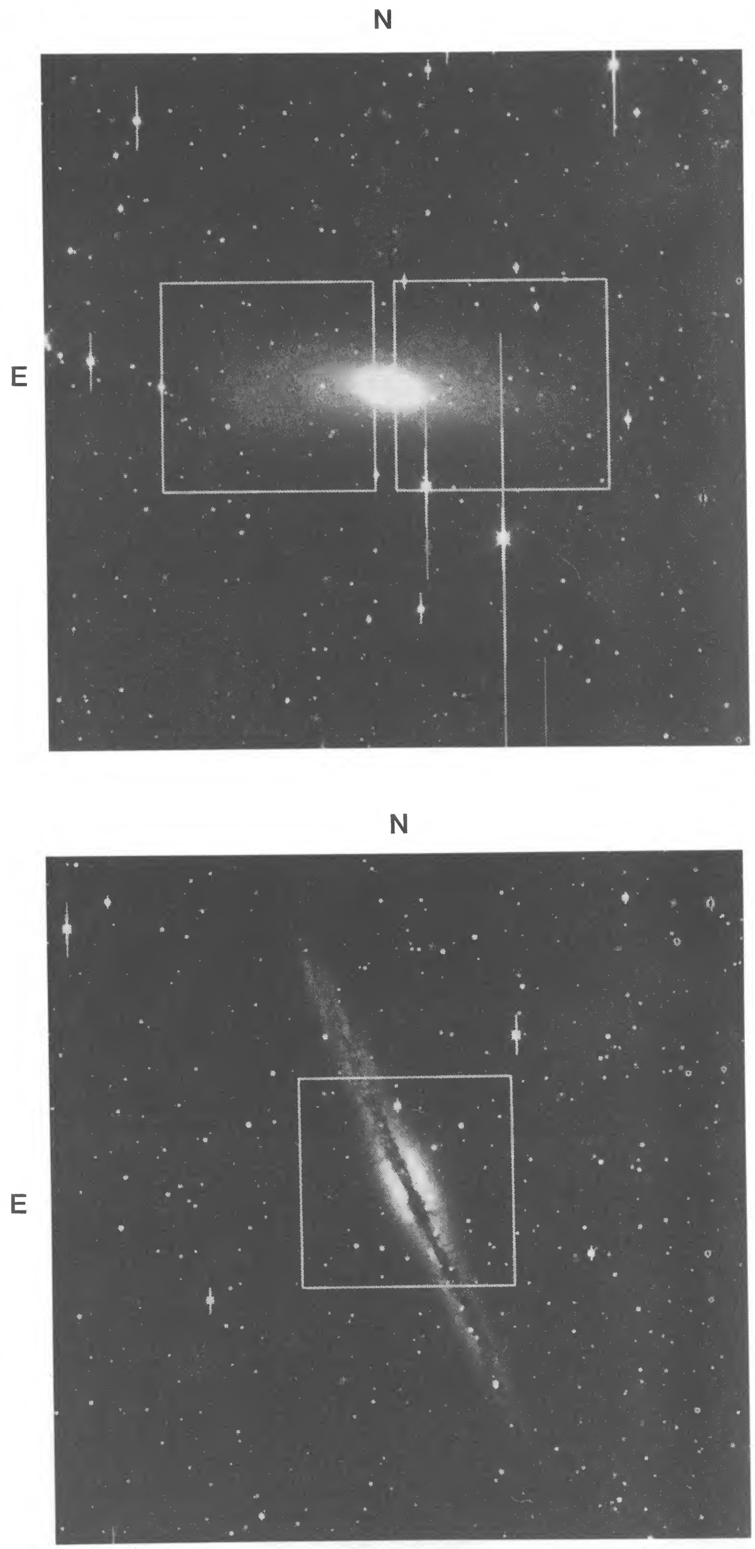

FIG. 1.—The survey fields in NGC 1023 and NGC 891 are shown overlain on wide-field (18'.4 × 18'.4) Tektronix 2048 × 2048 images taken with the Kitt Peak 4 m telescope. North is at the top, and east is to the left.

those of stars in the Space Telescope Guide Star Catalog. We then identified these secondary astrometric standards on our on-band sum CCD frames and measured the positions of the PN candidates relative to these stars. Despite the two-step process, we estimate the errors in our coordinates to be less than 1″.

Photometry of the PN candidates was performed as in Paper V. We first used the DAOPHOT photometry package (Stetson 1987) to determine the PSF for each field by measuring ~10 isolated stars on the on-band sum frames. We then used these PSFs to determine the instrumental λ5007 magnitudes of stars on the on-band frames, and PNs on the difference frames. To force the three fields of NGC 1023 onto a common photometric system, we took advantage of the overlap in the fields and calculated the least-squares condition required to match the magnitudes of stars contained on more than one CCD image (Ciardullo et al. 1987). We then placed the magnitudes on an absolute system by comparing 5″ aperture measurements of field stars with similar measurements made of five Stone (1977) and Oke (1974) spectrophotometric standards. Finally, we computed the standard magnitudes for the PNs by modeling the filter transmission curve (Paper III)

TABLE 2

NGC 1023 PLANETARY NEBULAE

ID	α(1950)	δ(1950)	m_{5007}	Sample	ID	α(1950)	δ(1950)	m_{5007}	Sample
1	2 37 09.34	38 50 54.6	25.47	S	56	2 37 21.28	38 51 54.7	26.51	
2	2 37 03.44	38 51 58.9	25.78	S	57	2 37 22.08	38 51 00.4	26.52	
3	2 37 23.06	38 50 36.2	25.79	S	58	2 37 31.95	38 52 38.5	26.53	
4	2 37 09.97	38 50 49.7	25.82	S	59	2 37 21.41	38 51 07.8	26.53	
5	2 37 19.25	38 51 44.6	25.83	S	60	2 37 06.70	38 51 23.5	26.56	
6	2 36 54.43	38 51 26.5	25.85	S	61	2 37 22.36	38 50 48.0	26.56	
7	2 37 18.89	38 51 00.1	25.90		62	2 37 23.53	38 50 50.1	26.57	
8	2 37 05.30	38 51 38.0	25.90	S	63	2 37 22.19	38 51 12.9	26.62	
9	2 37 17.59	38 50 41.1	25.97		64	2 37 30.54	38 50 44.2	26.63	
10	2 37 11.14	38 50 59.3	25.98		65	2 37 18.63	38 50 26.5	26.64	
11	2 37 17.74	38 50 18.4	26.00	S	66	2 36 59.09	38 49 48.1	26.64	
12	2 37 20.55	38 50 56.1	26.02		67	2 37 18.04	38 49 28.6	26.64	
13	2 37 24.58	38 51 58.4	26.02	S	68	2 37 12.86	38 51 18.7	26.65	
14	2 37 19.12	38 51 10.5	26.03		69	2 37 17.82	38 51 39.4	26.68	
15	2 37 03.98	38 50 40.5	26.04	S	70	2 37 34.82	38 49 47.5	26.68	
16	2 37 09.71	38 51 17.5	26.07	S	71	2 37 22.83	38 51 47.1	26.70	
17	2 37 20.63	38 51 09.1	26.10		72	2 37 07.91	38 52 28.1	26.70	
18	2 37 22.56	38 50 29.3	26.10	S	73	2 37 31.64	38 51 21.5	26.70	
19	2 37 19.41	38 50 59.4	26.12		74	2 37 29.60	38 51 12.4	26.70	
20	2 37 06.67	38 50 10.9	26.16	S	75	2 37 18.07	38 49 42.4	26.71	
21	2 37 27.49	38 50 35.6	26.16	S	76	2 37 31.12	38 51 59.0	26.73	
22	2 37 25.41	38 51 55.7	26.16	S	77	2 37 12.95	38 50 15.3	26.73	
23	2 37 08.77	38 52 54.0	26.17	S	78	2 37 06.45	38 50 25.6	26.83	
24	2 37 10.19	38 50 35.7	26.20	S	79	2 37 04.61	38 50 14.3	26.83	
25	2 37 06.36	38 51 43.9	26.20	S	80	2 37 09.84	38 51 58.0	26.83	
26	2 37 09.13	38 51 18.5	26.21	S	81	2 37 11.10	38 49 58.6	26.84	
27	2 37 11.18	38 50 55.1	26.23		82	2 37 12.01	38 51 17.2	26.90	
28	2 36 58.34	38 50 04.2	26.24	S	83	2 37 00.31	38 50 51.2	26.90	
29	2 37 12.15	38 50 22.1	26.26	S	84	2 37 12.68	38 49 34.2	26.91	
30	2 37 29.63	38 49 34.9	26.26	S	85	2 37 25.43	38 50 33.9	26.92	
31	2 37 06.78	38 50 24.0	26.28	S	86	2 37 04.97	38 52 19.5	26.92	
32	2 37 19.27	38 51 48.0	26.28	S	87	2 37 07.60	38 50 12.3	26.94	
33	2 37 26.24	38 51 12.2	26.29	S	88	2 37 05.32	38 51 06.5	26.95	
34	2 37 19.12	38 51 17.3	26.29		89	2 37 32.43	38 53 00.6	26.96	
35	2 37 10.13	38 51 06.0	26.30	S	90	2 37 01.55	38 49 58.0	27.02	
36	2 37 20.86	38 50 31.4	26.30	S	91	2 37 28.63	38 50 01.5	27.02	
37	2 37 24.52	38 51 20.8	26.32	S	92	2 37 08.95	38 50 07.1	27.03	
38	2 37 20.96	38 51 44.8	26.32	S	93	2 37 08.35	38 50 44.7	27.06	
39	2 37 06.44	38 51 02.2	26.33	S	94	2 37 05.47	38 50 01.6	27.09	
40	2 37 17.69	38 50 40.6	26.35		95	2 37 09.42	38 51 47.2	27.15	
41	2 37 02.89	38 51 01.2	26.36	S	96	2 37 12.20	38 52 14.5	27.17	
42	2 37 11.95	38 50 23.5	26.36	S	97	2 37 01.11	38 51 45.0	27.23	
43	2 37 34.12	38 50 53.0	26.39	S	98	2 37 26.55	38 50 52.6	27.25	
44	2 37 10.67	38 51 14.4	26.40	S	99	2 37 01.65	38 50 22.0	27.27	
45	2 37 19.31	38 50 19.8	26.42	S	100	2 37 12.30	38 49 26.7	27.30	
46	2 37 13.08	38 51 11.3	26.43		101	2 37 05.83	38 50 58.0	27.33	
47	2 37 21.08	38 50 51.2	26.44	S	102	2 37 08.22	38 49 12.9	27.37	
48	2 37 11.13	38 50 43.0	26.44		103	2 37 05.43	38 49 38.3	27.42	
49	2 37 31.77	38 50 55.2	26.45	S	104	2 37 08.12	38 50 40.5	27.49	
50	2 37 05.94	38 49 44.3	26.45	S	105	2 36 59.83	38 49 55.2	27.50	
51	2 37 29.77	38 50 10.8	26.45	S	106	2 37 30.29	38 52 01.6	27.60	
52	2 37 11.62	38 50 58.7	26.48		107	2 37 07.33	38 52 18.8	27.69	
53	2 37 07.84	38 50 08.0	26.48	S	108	2 37 06.18	38 52 04.4	27.74	
54	2 37 01.59	38 50 18.1	26.49	S	109	2 37 06.58	38 51 30.1	27.77	
55	2 37 08.13	38 50 02.0	26.49	S	110	2 37 30.21	38 50 21.6	27.82	

and using the photometric procedures for emission-line objects described by Jacoby, Quigley, & Africano (1987). For NGC 1023, we assumed a stellar rotation rate of 180 km s^{-1} (Sancisi et al. 1984) and a velocity dispersion of 80 km s^{-1} (Kormendy 1982). PNs in the halo of NGC 891 were assumed to have a velocity dispersion of 120 km s^{-1}, a number consistent with that observed for the spheroidal component of the Milky Way (Freeman 1983). We estimate that the combined uncertainty in our photometric zero points, due to errors in the standard star measurements and the narrow-band filter calibration, is 0.04 mag.

The equatorial positions and computed [O III] λ5007 magnitudes for the PNs in NGC 1023 and NGC 891 are presented in Tables 2 and 3. Table 3 also contains the measured z distance for the PNs in NGC 891. The mean internal photometric error of these measurements, as determined by DAOPHOT, is given as a function of magnitude in Table 4. Table 5 gives the coordinates of the brightest astrometric standard stars in our fields. Following Paper II,

$$m_{5007} = -2.5 \log F_{5007} - 13.74 . \quad (1)$$

3. DEFINING STATISTICAL SAMPLES

Figure 2 displays the raw PNLFs for NGC 1023 and NGC 891 binned into 0.2 mag intervals. The distributions are remarkably similar: despite the fact that the data are incomplete past $m_{5007} \approx 26.5$, the abrupt truncation of the PNLF at bright magnitudes is readily apparent. This, in itself, is strong evidence for the insensitivity of the PNLF cut-off to parent stellar population, since it is unlikely that the stars in the disk of an SB0 galaxy would have the same age and metal abundance as those in the halo of a late Sb.

In order to derive precise distances to NGC 1023 and NGC 891, statistically complete samples of PNs had to be selected. In NGC 891, this was not difficult. Normally the detectability of an extragalactic PN depends on both its magnitude and the surface brightness of the underlying galaxy. In NGC 891, however, objects superposed on the bright galactic disk were excluded to avoid confusion with H II regions. This being the case, the detectability of PNs in NGC 891 is not a strong function of background surface brightness, and the point of incompleteness could be estimated directly from the luminosity

TABLE 4

PLANETARY NEBULA PHOTOMETRIC ERROR VERSUS MAGNITUDE

Magnitude	Mean 1 σ Error
25.50	0.06
25.75	0.07
26.00	0.08
26.25	0.09
26.50	0.11
26.75	0.13
27.00	0.15
27.25	0.17
27.50	0.20

TABLE 3

NGC 891 PLANETARY NEBULAE

ID	α(1950)	δ(1950)	m_{5007}	z (arcsec)
1	2 19 29.13	42 08 10.4	25.78	26.3
2	2 19 22.92	42 05 28.0	25.89	25.9
3	2 19 24.95	42 08 24.8	25.99	22.3
4	2 19 30.43	42 08 04.2	26.00	42.2
5	2 19 20.96	42 07 13.4	26.03	35.5
6	2 19 30.64	42 09 13.8	26.08	17.0
7	2 19 18.38	42 06 11.4	26.08	38.0
8	2 19 19.54	42 07 07.5	26.09	47.9
9	2 19 20.42	42 06 28.0	26.10	23.4
10	2 19 24.03	42 06 02.6	26.17	23.8
11	2 19 23.06	42 08 08.1	26.18	35.3
12	2 19 21.03	42 06 44.7	26.23	23.6
13	2 19 26.78	42 09 11.3	26.26	21.7
14	2 19 24.58	42 05 53.7	26.27	32.9
15	2 19 18.55	42 05 41.7	26.28	24.6
16	2 19 26.20	42 06 36.5	26.29	32.9
17	2 19 20.96	42 06 51.1	26.35	26.8
18	2 19 20.81	42 06 22.6	26.36	17.3
19	2 19 27.79	42 07 03.3	26.39	38.7
20	2 19 27.43	42 07 23.5	26.39	27.1
21	2 19 25.74	42 06 12.4	26.42	37.6
22	2 19 19.20	42 08 48.5	26.42	90.7
23	2 19 25.58	42 05 47.9	26.48	45.5
24	2 19 24.32	42 08 42.1	26.48	35.6
25	2 19 24.97	42 08 38.6	26.56	27.5
26	2 19 29.05	42 07 48.4	26.66	34.1
27	2 19 18.17	42 05 51.3	26.66	32.2
28	2 19 28.88	42 06 50.6	26.71	54.9
29	2 19 19.83	42 06 36.1	26.72	32.6
30	2 19 19.09	42 06 03.8	26.86	27.6
31	2 19 24.39	42 06 20.3	26.86	20.5
32	2 19 20.45	42 06 21.0	26.89	20.4
33	2 19 30.18	42 08 47.2	27.46	22.8

TABLE 5

ASTROMETRIC REFERENCE STARS

Galaxy	ID	α(1950)	δ(1950)
NGC 1023	a	2 37 21.80	38 50 01.9
	b	2 37 23.84	38 49 40.2
	c	2 37 23.71	38 50 16.0
	d	2 37 30.64	38 49 42.5
	e	2 37 35.71	38 50 13.0
	f	2 37 34.98	38 51 23.0
	g	2 37 34.42	38 52 36.2
	h	2 37 29.69	38 52 37.2
	i	2 37 21.07	38 52 06.5
	j	2 37 19.18	38 51 39.5
	k	2 37 21.58	38 50 06.8
	l	2 37 12.28	38 49 54.7
	m	2 37 03.31	38 50 30.8
	n	2 37 00.92	38 50 47.3
	o	2 36 59.11	38 49 21.6
	p	2 36 58.94	38 51 33.6
	q	2 37 02.23	38 51 16.5
	r	2 36 57.66	38 50 56.4
	s	2 37 07.13	38 52 34.9
	t	2 37 09.74	38 50 55.2
	u	2 37 09.81	38 50 36.4
	v	2 37 08.37	38 49 23.8
	w	2 37 07.56	38 50 36.8
	x	2 37 07.22	38 51 13.1
	y	2 37 07.76	38 52 56.8
NGC 891	a	2 19 14.92	42 08 33.8
	b	2 19 15.78	42 06 00.4
	c	2 19 16.18	42 06 04.1
	d	2 19 24.79	42 05 48.8
	e	2 19 23.14	42 08 45.5
	f	2 19 27.26	42 06 41.8
	g	2 19 30.81	42 07 48.9
	h	2 19 27.44	42 05 27.9
	i	2 19 15.78	42 07 59.9
	j	2 19 30.83	42 06 23.2
	k	2 19 32.14	42 07 59.0

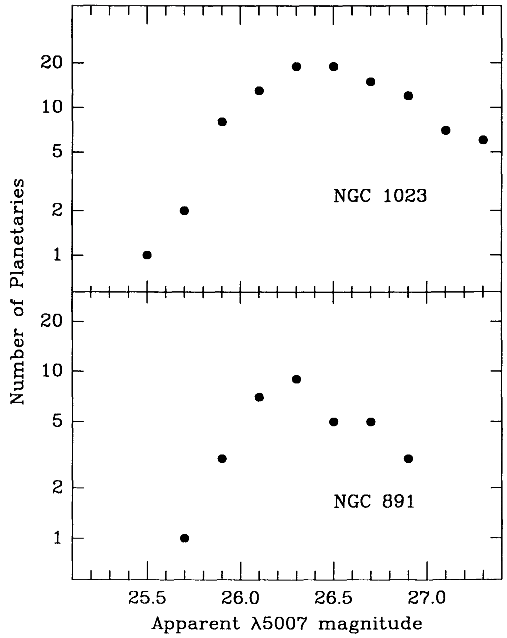

FIG. 2.—The raw PNLF for the SB0 galaxy NGC 1023 and the edge-on Sb spiral NGC 891 binned into 0.2 mag intervals. Magnitudes are defined as in Paper I, where $m_{5007} = -2.5 \log F_{5007} - 13.74$. Although the samples are heterogeneous and contain many objects past the nominal completeness limit of $m_{5007} \sim 26.4$, the similarity in the curves is obvious and again demonstrates the insensitivity of the PNLF cut-off to Hubble type. Note the one overluminous PN candidate in NGC 1023.

function histogram. From Figure 2, we estimate that the PN data in NGC 891 begin to become incomplete at $m_{5007} = 26.35$. The nine objects in Table 3 fainter than this limit have been excluded from further analysis.

To define the statistically complete sample of PNs in NGC 1023, we began by performing surface photometry on the galaxy. On 1990 November 28, we obtained a series of 10 minute B and V exposures of NGC 1023 using a Tektronix 1024 × 1024 CCD at the f/7.5 focus of the new Kitt Peak 0.9 m telescope. We then used DAOPHOT within IRAF to identify all the field stars within each frame and measure their magnitudes with PSF photometry. These stars were then removed using DAOPHOT's SUBSTAR option leaving only the wide field (11'.7 × 11'.7) image of the galaxy. We next used the surface photometry algorithms within the VISTA image processing system (Lauer, Stover, & Terndrup 1983) to exclude the irregular galaxy superposed on NGC 1023's disk and compute the primary galaxy's luminosity profile. These measurements were then placed on the standard system by comparing the counts per pixel in each elliptical isophote with large-aperture measurements made of 11 Landolt (1973, 1983) standard stars observed throughout the night.

Once the surface photometry of the galaxy was completed, the PNLF analysis proceeded as in previous papers in the series. First, the isophotal radial distance of each PN from the galaxy center was calculated by using the luminosity profile to find the semimajor axis of the isophote upon which it was superposed. The distribution of these distances was then compared to the isophotal distribution of galaxy light, corrected for the fraction of light enclosed in the survey regions. Since the luminosity-specific PN number density is approximately invariant over the face of a galaxy (Renzini & Buzzoni 1986; Paper II), this comparison yielded the completeness of the sample. This is displayed in Figure 3. PNs with $m_{5007} < 26.9$ follow the light extremely well in the outer part of the galaxy, but their luminosity-specific density begins to decline within $\sim 120''$ (isophotal radius) of NGC 1023's nucleus, due to the increased surface brightness of the galaxy background. For a brighter sample of PNs, those with $m_{5007} < 26.5$, this incompleteness does not become important until an isophotal radius of $\sim 50''$ is reached. While either of these samples can be used to derive a PNLF distance, the latter is slightly better for a distance determination. PNLF distances depend more on the photometry of the brightest planetaries than the faintest; hence, the inclusion of additional bright PNs at the expense of fainter objects improves the fits slightly. Similarly, slight errors in estimating the precise limits for incompleteness do not significantly affect the PNLF distance calculation.

After excluding those objects close to the NGC 1023's nucleus and fainter than $m_{5007} = 26.5$, 42 PNs remained in our sample. These are noted in Table 2 with an " S."

4. THE DISTANCE TO THE NGC 1023 GROUP

PNLF distances are derived by fitting the observed luminosity function of PNs within a galaxy to an empirical function. Based on PN measurements in the bulge of M31 (Paper II), M81 (Paper III), and the Leo I Group galaxies NGC 3377, NGC 3379, and NGC 3384 (Paper IV), Paper II proposed that the PNLF is well-represented by an equation of the form

$$N(M) \propto e^{0.307M}[1 - e^{3(M^* - M)}] , \qquad (2)$$

with $M^* = -4.48$. Such an equation combines the rising expo-

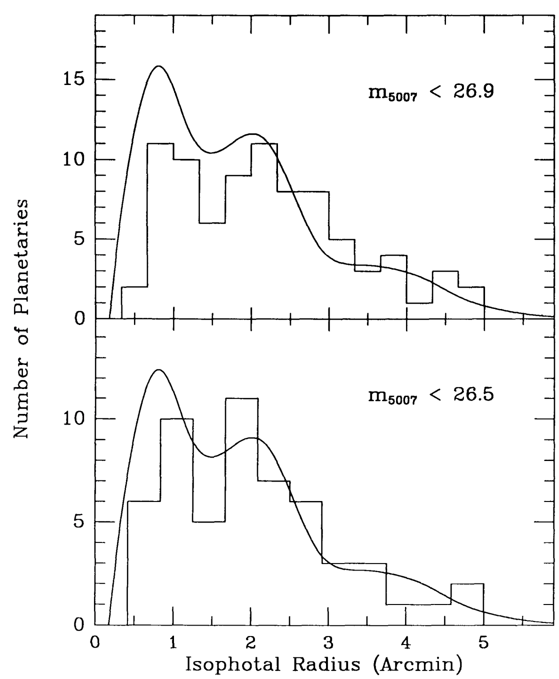

FIG. 3.—A histogram showing the distribution of isophotal radii for PN candidates in NGC 1023 with $m_{5007} < 26.5$, and with $m_{5007} < 26.9$. The solid lines display the amount of V luminosity surveyed, again vs. isophotal radius. A comparison of these distributions shows that within 60″ of NGC 1023's nucleus, incompleteness is important in both samples, as PNs are being lost amid the bright background of the galaxy. Between 60″ and 120″, however, only the bright PN sample appears to be complete. As with all galaxies surveyed for PNs, once outside the area of incompleteness, the distribution of PNs follows that of the light reasonably well.

nential of Henize & Westerlund (1963) and Jacoby (1980) with a bright-end exponential cut-off at M^*. Unfortunately, observations in the Virgo Cluster (Paper V) have shown that the PNLF cut-off, though hard, is not absolute—perhaps $\sim 1\%$ of all [O III] sources brighter than $M^* + 2.5$ are in a high-luminosity tail which extends at least 1.2 mag past M^*. Some of these sources may be due to the chance superposition of two bright PN candidates, but whether the remaining overluminous objects are indeed PNs or some other high-excitation emission-line sources is still subject to debate (see § 6). This tail is somewhat important in the present program, since, as Figure 2 and Table 2 demonstrate, NGC 1023 possesses an overluminous object. PN candidate No. 1 in NGC 1023 is over 0.3 mag more luminous than any other PN in the group. Since the empirical luminosity function of Paper II does not provide for the existence of these overluminous [O III] λ5007 sources, we chose to omit this object from our PN sample. Fortunately, because the luminosity function of PNs is so well-defined, this omission does not significantly affect the derived distance to the galaxy.

Before calculating the distance to NGC 1023 and NGC 891, an estimate of the interstellar extinction affecting the [O III] λ5007 magnitudes is needed. Internal extinction is not a problem in either galaxy: NGC 1023 is an SB0 galaxy with little, if any, star formation, and the only PNs considered in NGC 891 are those high above the galactic plane. However, the NGC 1023 Group as a whole is at low Galactic latitude ($b^{\rm II} \sim -19°$) and foreground extinction to the cluster is not negligible. Unfortunately, there is at present no way of knowing the precise reddening applicable to each galaxy. For NGC 1023, the formulas of Sandage (1973), Burstein & McDonald (1975), and de Vaucouleurs, de Vaucouleurs, & Corwin (1976; RC2) yield differential $E(B-V)$ extinctions of 0.068, 0.133, and 0.124, respectively; for NGC 891, these formulas give values of 0.077, 0.147, and 0.124. Rather than use any of these global formulas, we chose to adopt the total B band extinctions of Burstein & Heiles (1984), which are based on the measurement of Galactic H I. When we combine these numbers with Seaton's (1979) expression for extinction as a function of wavelength [$A_{5007} = 0.89E(B-V)$], we get a total λ5007 extinction of 0.222 mag toward NGC 1023 and 0.267 mag toward NGC 891. It should be noted, however, that the Burstein & Heiles extinction estimates are lower than those given by any of the global formulas, and any uncertainty in this value propagates directly into the distance determination. The adoption of the RC2 expression for extinction, for example, would immediately decrease all our derived distances by $\sim 10\%$.

We calculated the distances to NGC 1023 and NGC 891 and the formal uncertainties of the fits by using the maximum likelihood formulations of Paper II. The best-fit luminosity functions are drawn in Figure 4, and the results of the maximum likelihood analyses are displayed in Figure 5. It is immediately obvious that the PNLF method does indeed place the galaxies at the same distance, thus confirming the insensitivity of the PNLF to galaxy Hubble type. The most likely distance modulus of NGC 891 is $29.97^{+0.07}_{-0.11}$, which corresponds to a distance of $9.9^{+0.3}_{-0.5}$ Mpc. NGC 1023 has a true distance modulus of $29.97^{+0.05}_{-0.08}$ and is at a distance of $9.9^{+0.2}_{-0.3}$ Mpc. (This distance shrinks to 9.1 Mpc if our empirical model is forced to include PN No. 1. However, the quality of this fit is poor, and the implied distance disagrees with that found from other statistical samples of PNs in the galaxy.) For an angular

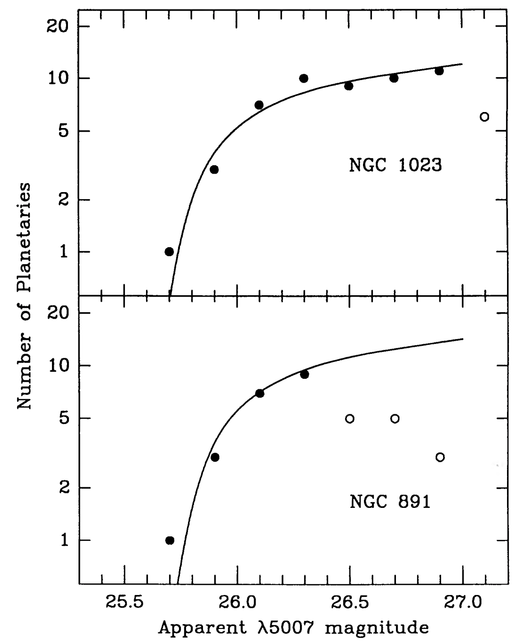

FIG. 4.—The PNLFs for NGC 1023 and NGC 891 derived from complete samples of PNs within both galaxies. The data are binned into 0.2 mag intervals. The solid lines show the empirical PNLF convolved with the mean photometric error vs. magnitude relation and translated to the most likely apparent distance modulus of each galaxy. Open circles show PNs below the completeness limit which have not been included in the fit. To demonstrate the insensitivity of PNLF distances to the precise choice of PN samples, the NGC 1023 plot compares the luminosity function of a faint sample of PNs ($m_{5007} <$ 26.9) with the most likely empirical PNLF derived from a brighter PN sample ($m_{5007} <$ 26.5). The two distributions are in perfect agreement.

separation of 4°.7 on the sky, these distances imply a true spatial separation of 0.8 Mpc, well within the size of a typical cluster. The distances are also in good agreement with the group distance modulus of 29.98 ± 0.25 determined from the B

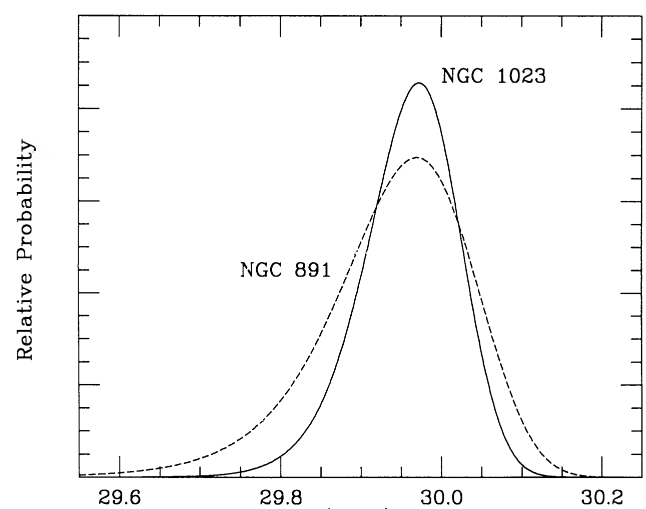

FIG. 5.—The results from the maximum likelihood analysis for the PNLFs of NGC 1023 and NGC 891. The abscissa is the true distance modulus; the ordinate is the probability that the observed PNLF is drawn from the empirical model (Paper II) at the given distance. Corrections for extinction and photometric error have been applied. The most likely distances for the two galaxies are identical, confirming that the two galaxies are indeed within a common cluster.

band and H band Tully-Fisher relations (Aaronson & Mould 1983; Bottinelli et al. 1986; Pierce 1991).

The uncertainties quoted above are the 1 σ internal measurement uncertainties only. To estimate the true errors in our measurement, we must combine these internal uncertainties with that of our standard star measurements and filter calibration (0.04 mag from § 2), the definition of the PNLF (0.05 mag; see Paper II), the adopted distance and extinction to M31 (0.10 mag), and the foreground extinction (0.05 mag; Burstein & Heiles 1984). This results in a total 1 σ error of 0.14 mag for NGC 1023 and 0.16 mag for NGC 891. However, we caution that these estimates assume that all our errors are random. Possible systematic errors in the Galactic extinction or in the distance to M31 are not included in this calculation.

5. IMPLICATIONS FOR STELLAR EVOLUTION

Aside from information as to distance, a PNLF maximum likelihood analysis also produces information on the total number of PNs within a galaxy, and, by inference, the evolutionary flux of the underlying stellar population. Renzini & Buzzoni (1986) have noted that, when normalized to bolometric luminosity, the number of stars evolving through any phase of stellar evolution should be insensitive to age, metallicity, or initial mass function. This being the case, the number of PNs detected in a galaxy should depend only on the underlying galaxy's luminosity, and not on properties such as its color, metallicity, or UV flux. If the luminosity-specific PN density is seen to correlate with such properties, then the models for the late stages of stellar evolution would have to be reexamined.

We calculated NGC 1023's luminosity-specific PN number density following the procedure outlined in Paper II. We first used the galaxy's V band luminosity profile computed in § 3 to find the total V luminosity contained within our survey fields, excluding the region of incompleteness and the superposed irregular galaxy. We then corrected this value for the Galactic extinction and computed the applicable bolometric correction based on the *UBVRIJHK* colors of Frogel et al. (1978) and de Vaucouleurs & Longo (1984). The resulting bolometric luminosity was then used to normalize our maximum likelihood solution and produce $\alpha_{2.5}$, the number of PNs within 2.5 mag of M^* per unit bolometric luminosity. For NGC 1023, this number is $22^{+4}_{-3} \times 10^{-9}\, L_{\odot}^{-1}$.

Figure 6 plots the luminosity-specific PN density versus $U - V$ color, metallicity, and ultraviolet color for 10 galaxies with reasonably well-determined values of α. It is immediately obvious that, although α may be weakly correlated with metallicity and ultraviolet flux, the apparent PN production rate correlates strongly with the $U - V$ color index. The sense of the correlation, which was first noted by Peimbert (1990), is that blue galaxies produce more PNs per unit bolometric luminosity that galaxies with a redder population. This trend is opposite that predicted by the models of Renzini & Buzzoni (1986): in their calculations, a population's luminosity-specific stellar death rate slowly increases with age.

There are two straightforward interpretations to this anticorrelation. The first, which has been discussed in Peimbert (1990), is to presume that [O III]–bright PNs are formed by relatively young stars, and that as the percentage of young stars in a galaxy decreases, the galaxy becomes redder and α decreases. Although possible, the observations NGC 891 make this scenario unlikely. Because no surface photometry exists for NGC 891's outer bulge and halo, an accurate determination of α for this region is impossible. However, as Figure 2 illustrates, a substantial population of [O III]–bright halo objects clearly does exist. If NGC 891's spheroid is anything like that of the Milky Way, virtually all the stars in this region are old. Since there is no young population to make [O III]–bright PNs in the outer bulge, a two-population model cannot be used to explain the observations.

A second method of explaining the correlation seen in Figure 6 is to propose that as a stellar population grows older and redder, the percentage of stars that form [O III] bright PNs declines. This can happen if a population of stars with a single turnoff mass produces remnants with a range of core masses. Support for this scenario comes from observations of Galactic clusters and from the PNLF itself. By observing white dwarfs in open clusters, Weidemann & Koester (1983) have shown that when a population ages, the stars turning off the main sequence produce remnants with lower and lower final masses. The invariance of the PNLF to color, however, demonstrates that this relation cannot hold for all stars. In every population, at least some stars form [O III] bright PNs, and, as shown by Jacoby (1980; hereafter Paper I), these bright objects can only be made by high-mass cores. Stellar evolution *is* reflected in the relative number of [O III] bright PNs, however—the older a system is, the fewer bright PNs are seen. If a single turnoff mass produces a distribution of core masses,

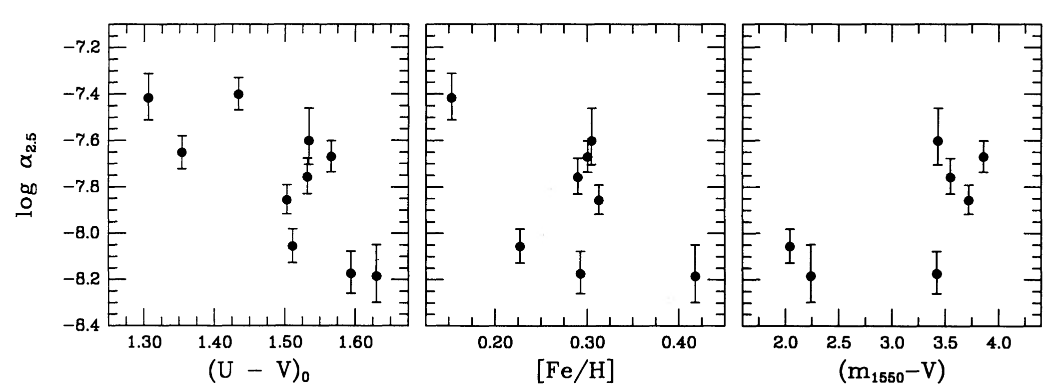

FIG. 6.—A plot of the luminosity-specific PN density vs. color (*left*), metallicity (*center*), and ultraviolet color (*right*) for 10 galaxies with measured PNLFs (NGC 1023, 3115, 3377, 3379, 3384, 4374, 4406, 4472, 4486, and 4649). The optical colors are from Poulain (1988), Michard (1982), and Frogel et al. (1978); the metallicities are based on the Terlevich et al. (1981) calibration of the Mg_2 data of Davies et al. (1987); and the ultraviolet colors are from Burstein et al. (1988). The error bars represent the formal uncertainty of the maximum likelihood fits and do not include systematic errors in the luminosity normalizations. The trends suggest that the production rate of bright PNs depends on stellar population, with younger populations producing more PNs.

and if the [O III] λ5007 emission from high-mass cores is artificially truncated, either by nebular abundance variations or by evolutionary time scale considerations (see § 7), then the Weidemann & Koester dependence would produce a correlation between α and color that is very similar to that observed. Moreover, since the lifetime of a PN central star depends very strongly on its mass ($\tau \propto M^{-9.6}$), any population which produces a large number of low-mass central stars may build up a sizable population of UV bright cores. Thus, an inverse correlation between α and $(m_{1550} - V)$ color is also explained by this kind of model.

Although the correlations presented in Figure 6 appear highly significant, it should be noted that the plotted error bars reflect only the formal uncertainties in the maximum likelihood fits and do not include systematic errors in the luminosity normalizations. These errors may be important. While PNLF distances are insensitive to mistakes made in estimating the PN detection limits, the same cannot be said of α. For example, if PNs within 60″ of a galaxy's nucleus cannot be detected due to the bright galaxy background, but the inner radius of incompleteness is misestimated to be at 30″, then a significant error will be made in the luminosity normalization. Because only a few PNs will be affected by such a mistake, this type of error does not significantly affect the derived PNLF distance determinations. The luminosity-specific PN number density will be affected, however, and an underestimate of the true value of α will be the result. Because of the difficulty in measuring precise completeness limits and calculating accurate bolometric corrections, we estimate our values for α are accurate to ~30%. Since the correlation of α with $U - V$ color extends over a factor of 10 in PN density, we believe this correlation to be real. However, a larger sample of galaxies is still needed to confirm the trend.

6. OVERLUMINOUS OBJECTS

The existence of an overluminous emission-line object in NGC 1023 affords us an opportunity to evaluate the true nature of these objects. Overluminous λ5007 sources were first identified in the elliptical and S0 galaxies of Virgo (Paper V). At that time, we dismissed the possibility that these objects could be small H II regions due to the lack of evidence for star formation in these galaxies. However, in light of the NGC 1023 Group data, this possibility should be reexamined.

In our first pass at identifying PN candidates in NGC 1023, one object stood out from the rest. Although in most respects the candidate appeared normal, its luminosity was 0.5 mag brighter than any other PN candidate in the group. It was only by closely examining the image on our best (0″.8) seeing frame that we could tell that the object was slightly extended, and hence was not a true PN (see Fig. 7, right panel). If NGC 1023 were at the distance of Virgo, or if the seeing were slightly poorer, we would not have been able to eliminate this object on the basis of its image profile or Hα flux, and its nature would have remained a mystery in line with the Virgo objects. As it is, the object has a diameter of ~40 pc and is just large enough to be resolved. PN candidate No. 1 may be a similar object that is slightly less extended.

If the overluminous objects are indeed H II regions, it would imply that at least some star formation is occurring in this SB0 galaxy. For NGC 1023, this is a plausible hypothesis: the galaxy is embedded in a large gas cloud, which contains $1.5 \times 10^9\ M_\odot$ of neutral hydrogen (Sancisi et al. 1984). It is possible that some of this gas is being converted into stars, forming a small population of [O III]–bright emission–line sources. However, another possibility is that these objects are not H II regions at all, but are instead supernova remnants. This possibility was also dismissed in the Virgo study. For normal elliptical and S0 galaxies, the interstellar medium has such a low density that little, if any, material can be swept up, and thus the lifetime of a remnant is short. For a gas-rich system such as NGC 1023, however, the possibility of a long-lived remnant cannot be ignored.

Another object in NGC 1023 confirms the suggestion raised in Paper V that some of these objects are, in fact, chance super-

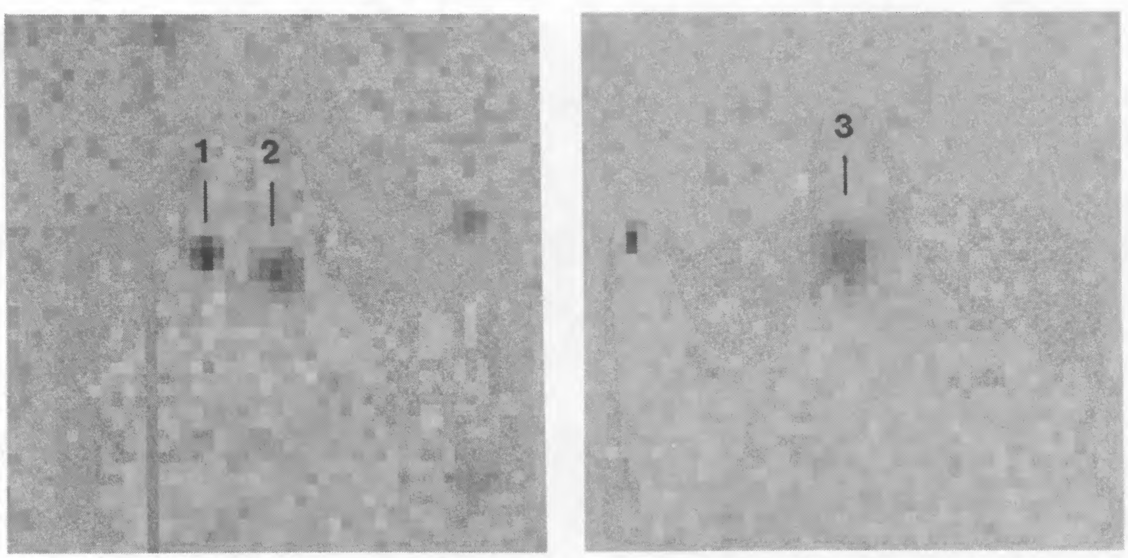

FIG. 7.—An enlargment of two regions in our best frame of NGC 1023. The left panel demonstrates the PSF for a single bright PN (object 1). Note that the image is nearly undersampled by the 0″.3 pixels of the TI2 CCD during this exposure (~0″.8 seeing). A nearby overluminous candidate (object 2) appears to be a chance superposition of two objects separated by roughly 0″.6. The object in the right panel (object 3) was initially identified as an overluminous PN, but its profile extends across 5–6 pixels which clearly exceeds that of object 1.

positions of two bright PNs. The left panel of Figure 7 depicts an example of a PN candidate which, under poorer seeing conditions, would have certainly been called overluminous. Although the relative proximity of NGC 1023 and the excellent seeing conditions allowed us to resolve the candidate into two objects, such would not have been the case had we been observing galaxies in Virgo. For more distant galaxies it is therefore expected that more overluminous objects will be found.

7. IMPLICATIONS FOR FUTURE DISTANCE MEASUREMENTS

The key question about the PNLF, as with all other stellar-based extragalactic standard candles, is its dependence on stellar population. The PNLF distances derived in the Leo I Group (Paper IV) and in the Virgo Cluster (Paper V) showed no significant correlation with galaxy luminosity, color, metallicity, or Hubble type, but these galaxies were all metal-rich ellipticals or S0s, and thus sampled only a limited range of stellar parameters. In Paper VI, an extreme population was sampled, that of the Large Magellanic Cloud. Although the stars in the LMC are younger and more metal-poor than those in any of the previously studied galaxies, the PNLF method still produced a distance that was in perfect agreement with that determined by other methods.

In this paper, we have again sampled two very different stellar populations. At its derived distance of 9.9 Mpc, 1″ in NGC 891 corresponds to 47.8 pc; thus, the PNs observed in this galaxy are all at least 800 pc from the galactic plane, and most have z-distances greater than 1.3 kpc. Since the analogous stars in the Milky Way primarily belong to the Galaxy's spheroidal component, it is reasonable to assume that the PNs surveyed in NGC 891 originate from a population older than ~ 10 Gyr (Mihalas & Binney 1981). The stars in NGC 1023's disk, however, are considerably younger than this, with ages determined from differential population synthesis of only ~ 3 Gyr (Gregg 1989). Yet the derived distance to NGC 1023 is identical with that of NGC 891. Based on this, it appears that a population's age or turn-off mass has little effect on the cut-off of the PNLF.

The PNLF's invariance to the turn-off mass of a stellar population is hard to explain. Most mass-loss laws suggest that the mass of a PN central star depends somewhat on the initial mass of the progenitor, but the PNLF observations in Leo, Virgo, the NGC 1023 Group, and in the LMC prove that this dependence is virtually nonexistent for intermediate and late-type stars. Weidemann & Koester's (1983) measurements of white dwarf masses suggest that this might be the case, but the scatter is too large to say anything definitive. A possible explanation can be inferred from the results of Kaler & Jacoby (1991) who show that high-mass central stars are absent from samples of bright PNs. This suggests that central star evolutionary rates are so rapid for massive stars that they do not contribute to the observed samples of bright extragalactic PNs. If this is the case, then a stellar population that has a high turn-off mass will produce a sample of bright PNs with essentially the same upper luminosity limit as a population with a lower turn-off mass.

An alternative explanation for the constancy of the PNLF cut-off is suggested by the nitrogen to oxygen abundance ratio observed in Galactic and Magellanic Cloud PNs. Kaler & Jacoby (1990; 1991) have noted that as a function of core mass, the N/O abundance ratio in PNs is relatively constant for $M_c \lesssim 0.65\ M_{\odot}$. At larger core masses, however, nitrogen is dramatically increased relative to oxygen, possibly as a result of CNO-burning in the progenitor envelopes. If this is true, it implies that high-mass stars may not produce [O III]–bright PNs, due to the increased cooling efficiency of other species.

Including the NGC 1023 Group, internal PNLF tests now exist in three clusters and include galaxies which span Hubble types from E0 to Sb. External tests against distances determined by other methods have been performed on two additional galaxies, the Sb spiral M81, and the Large Magellanic Cloud (type Sdm/Im). In these surveys, no galaxy has yet been found with a discordant distance determination, and no systematic behavior with any external parameter has been seen. Based on these facts, we believe PNs are currently the best extragalactic standard candles for measuring distances outside the Local Group.

REFERENCES

Aaronson, M., & Mould, J. 1983, ApJ, 265, 1
Bottinelli, L., Gougenheim, L., Paturel, G., & Teerikorpi, P. 1986, A&A, 156, 157
Burstein, D., Bertola, F., Buson, L. M., Faber, S. M., & Lauer, T. D. 1988, ApJ, 328, 440
Burstein, D., & Heiles, C. 1984, ApJS, 54, 33
Burstein, D., & McDonald, L. H. 1975, AJ, 80, 17
Capaccioloi, M., Lorenz, H., & Afanasjev, V. L. 1986, A&A, 169, 54
Ciardullo, R., Ford, H. C., Neill, J. D., Jacoby, G. H., & Shafter, A. W. 1987, ApJ, 318, 520
Ciardullo, R., Jacoby, G. H., & Ford, H. C. 1989, ApJ, 344, 715 (Paper IV)
Ciardullo, R., Jacoby, G. H., Ford, H. C., & Neill, J. D. 1989, ApJ, 339, 53 (Paper II)
Davies, R. L., Burstein, D., Dressler, A., Faber, S. M., Lynden-Bell, D., Terlevich, R. J., and Wegner, G. 1987, ApJS, 64, 581
de Vaucouleurs, G. 1975, in Stars and Stellar System, Vol. 9, Galaxies and the Universe, ed. A. Sandage, M. Sandage, & J. Kristian (Chicago: Univ. Chicago Press), 557
de Vaucouleurs, G., de Vaucouleurs, A., & Corwin, H. G. Jr. 1976, Second Reference Catalogue of Bright Galaxies (Austin: Univ. Texas Press) (RC2)
de Vaucouleurs, A., & Longo, G. 1988, Catalogue of Visual and Infrared Photometry of Galaxies (Austin: Univ. Texas)
Feast, M. W., & Walker, A. R. 1987, ARA&A, 25, 345
Freedman, W. L., & Madore, B. F. 1988, ApJ, 332, L63
Freeman, K. C. 1983, in IAU Symposium 106, The Milky Way Galaxy, ed. H. van Woerden, R. J. Allen, & W. B. Burton (Dordrecht: Reidel), 113
Frogel, J. A., Persson, S. E., Aaronson, M., & Matthews, K. 1978, ApJ, 220, 75
Gregg, M. D. 1989, ApJ, 337, 45
Henize, K. G., & Westerlund, B. E. 1963, ApJ, 137, 747
Huchra, J. P., & Geller, M. J. 1982, ApJ, 257, 423
Jacoby, G. H. 1980, ApJS, 42, 1
———. 1989, ApJ, 339, 39 (Paper I)
Jacoby, G. H., Ciardullo, R., & Ford, H. C. 1990, ApJ, 356, 332 (Paper V)
Jacoby, G. H., Ciardullo, R., Ford, H. C., & Booth, J. 1989, ApJ, 344, 704 (Paper III)
Jacoby, G. H., Quigley, R. J., & Africano, J. L. 1987, PASP, 99, 672
Jacoby, G. H., Walker, A. R., & Ciardullo, R. 1990, ApJ, 365, 471 (Paper VI)
Kaler, J. B., & Jacoby, G. H. 1990, ApJ, 362, 491
———. 1991, ApJ, 372, 215
Kormendy, J. 1982, ApJ, 257, 75
Landolt, A. U. 1973, AJ, 78, 959
———. 1983, AJ, 88, 439
Lauer, T. R., Stover, R. J., & Terndrup, D. 1983, The VISTA User's Guide (Lick Obs. Tech. Rept. No. 34) (Santa Cruz: Univ. of California at Santa Cruz)
Michard, R. 1982, A&AS, 49, 591
Mihalas, D., & Binney, J. 1981, Galactic Astronomy (San Francisco: Freeman)
Oke, J. B. 1974, ApJS, 27, 21
Osterbrock, D., & Sharpless, S. 1952, ApJ, 115, 140
Peimbert, M. 1990, Rev. Mexicana Astron. Ap., 20, 119
Pierce M. 1991, private communication
Pierce, M. J., & Tully, R. B. 1988, ApJ, 330, 579
Pottasch, S. R. 1990, A&A, 236, 231
Poulain, P. 1988, A&AS, 72, 215

Rand, R. J., Kulkarni, S. R., & Hester, J. J. 1990, ApJ, 352, L1
Reid, M. J. 1989, in IAU Symposium 136, The Center of the Galaxy, ed. M. Morris (Dordrecht: Kluwer), 37
Renzini, A., & Buzzoni, A. 1986, in Spectral Evolution of Galaxies, ed. C. Chiosi & A. Renzini (Dordrecht: Reidel), 195
Sancisi, R., van Woerden, H., Davies, R. D., & Hart, L. 1984, MNRAS, 210, 497
Sandage, A. 1973, ApJ, 183, 711
Seaton, M. J. 1979, MNRAS, 187, 73P
Stetson, P. 1987, PASP, 99, 191
Stone, R. P. S. 1977, ApJ, 218, 767
Terlevich, R., Davies, R. L., Faber, S. M., & Burstein, D. 1981, MNRAS, 196, 381
Tully, R. B., & Pierce, M. 1989, private communication
Tully, R. B. 1988, Nearby Galaxies Catalog (Cambridge: Cambridge Univ. Press)
van der Kruit, P. C. 1984, A&A, 140, 470
Weidemann, V., & Koester, D. 1983, A&A, 121, 77
Welch, D. L., McLaren, R. A., Madore, B. F., & McAlary, C. W. 1987, ApJ, 321, 162